Flexural Strength of Fiber Cementitious Composites

By Mohamed Maalej,[1] and Victor C. Li,[2] Members, ASCE

Abstract: An analytical model has been developed for the flexural strength of fiber-reinforced cement-based materials. The proposed model adopts the fictitious crack concept to relate the flexural strength of these fiber composites to their tension-softening properties and to specimen geometry. For the case of a cementitious matrix reinforced with discontinuous randomly distributed fibers, the flexural strength can be related to the micromechanical parameters and specimen geometry. A reasonable agreement has been observed between the model prediction and experimental data reported in literature, supporting the validity of the proposed model. This model led to conclude that the flexural strength of fiber cementitious composites is dependent on specimen geometry and is also strongly influenced by the stress acting across the process zone. In addition, the flexural strength is always higher than the tensile strength and it is reached when the fracture process zone is only partially developed. The model can be used to design fiber cementitious composites for optimum flexural strength.

INTRODUCTION

The flexural strength of unreinforced cement-based materials and their fiber composites is important for many current applications such as road slabs, airfield runways, roofing tiles, sewage pipes, and architectural wall panels. In addition, using a simple flexure test, an important property of cement-based materials, namely their tensile strength, can be deduced from their flexural strength if the latter can be related to the former through an analytical or numerical model.

It is well accepted that the flexural strength of cement-based materials is greater than their uniaxial tensile strength. In addition, the flexural strength of these materials is not a constant but depends on the specimen geometry. Hillerborg et al. (1976) showed, for the first time, that the flexural strength of concrete depends on a parameter called the brittleness ratio, which is a function of both material properties and specimen geometry. In particular, they showed that the flexural strength of concrete depends on the material fracture resistance, which can be described by a stress crack-opening law called the tension-softening relationship. In their analysis they introduced a new fracture-mechanics approach called the "fictitious crack model" (FCM).

In an uncracked section, the FCM assumes that fracture zones start to develop at locations where the maximum principle stress reaches the tensile strength of the material. When a crack forms, the stress at the crack mouth is not assumed to fall to zero immediately, instead, it is assumed to decrease with increasing crack opening according to the tension-softening relationship. The stress is assumed to fall to zero only when the crack-mouth opening

[1]Grad. Res. Asst., ACE-MRL, Dept. of Civ. and Envir. Engrg., Univ. of Michigan, Ann Arbor, MI 48109-2125.

[2]Prof., ACE-MRL, Dept. of Civ. and Envir. Engrg., Univ. of Michigan, Ann Arbor, MI.

Note. Discussion open until January 1, 1995. To extend the closing date one month, a written request must be filed with the ASCE Manager of Journals. The manuscript for this paper was submitted for review and possible publication on May 17, 1993. This paper is part of the ***Journal of Materials in Civil Engineering***, Vol. 6, No. 3, August, 1994. ©ASCE, ISSN 0899-1561/94/0003-0390/$2.00 + $.25 per page. Paper No. 6190.

reaches a critical value w_c. The portion of the crack, where the crack width is less than w_c, corresponds to a microcracked zone with some remaining ligaments for stress transfer. For this reason, this portion of the crack is called the "fictitious crack," or more generally the cohesive or process zone; and the remaining portion is called the "real crack."

Hillerborg et al. (1976) combined the FCM with finite-element analysis to determine the ultimate flexural moment capacity of unreinforced concrete beams loaded in pure bending. A linear tension-softening relationship was assumed. Their results indicated that the ultimate moment is reached when the fracture process zone is only partially developed. The analysis of Hillerborg et al. (1976) led to an explanation of the difference between flexural strength and tensile strength, and the dependence of flexural strength on the geometry of the specimen, namely the specimen depth. Specifically, the flexural strength of a nonideally brittle material (or quasi-brittle material) is strongly influenced by the stress acting across the process zone, and decreases with specimen depth. The latter is an example of what is increasingly recognized as size effect in concrete structures (Bažant 1992).

Zhu (1990) derived an analytical model for the flexural strength of concrete beams based on the Hillerborg fictitious crack model. In the derivation, Zhu assumed a linear tension-softening curve. The model results were in good agreement with the earlier finite-element method (FEM) analysis of Gustafsson (1985). Such an analytical model provides a simple way of computing the ultimate moment capacity of concrete beams and allows useful parametric studies to be performed such as the effect of specimen geometry, without resorting to numerical techniques.

In this study, the FCM concept was adopted to derive an analytical model for the flexural strength of fiber-reinforced cementitious composite beams. The tension-softening relationships for these composites have been related to the material's micromechanical parameters (such as fiber length, fiber diameter, fiber tensile strength, fiber/matrix interfacial bond strength, and fiber and matrix elastic moduli) through explicit analytical expressions taking into account the effect of fiber rupture (Li 1992; Maalej et al., in press, 1993). Therefore, it is the purpose of this study to relate the flexural strength of these composites to the material's micromechanical parameters and the geometry of the specimen, through an explicit analytical model. The derived model can then be used to optimize the flexural strength of fiber-reinforced cementitious composites. The effect of fiber rupture is also taken into account in the derivation.

DERIVATION OF FLEXURAL STRENGTH FORMULA

Consider a rectangular beam, made of a fiber-reinforced cementitious composite and having a width b and depth d, loaded in bending. The reinforcing fibers have a diameter d_f, length L_f, tensile rupture strength σ_{fu}, and volume fraction V_f. The fiber/matrix interface has a bond strength τ and a snubbing friction coefficient f [the snubbing friction coefficient is an interface material parameter that characterizes a local frictional effect, called snubbing, resulting from the misalignment between the axis of a fiber bridging a matrix crack and the loading axis (Li et al. 1990)]. Fig. 1 shows the portion of this beam subjected to the highest bending moment M. A fictitious crack of length a and mouth opening w is assumed to have formed on the beam-tensile face.

Within the fracture process zone, the stress σ at any point x, is related

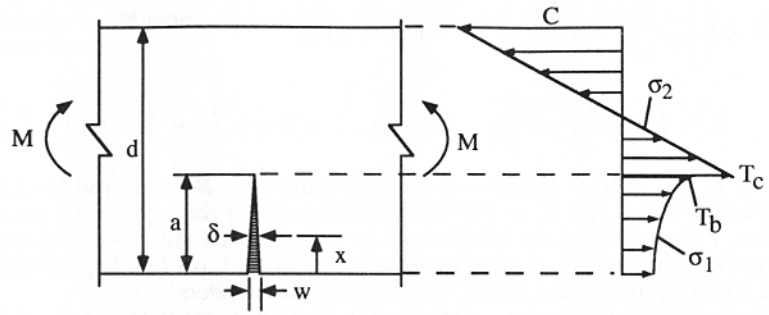

FIG. 1. Distribution of Normal Stresses in Critical Beam Section

to the width δ of the fictitious crack at that point by the following tension-softening relationship:

$$\sigma(\delta) = T_b \left[1 - 2k \left(\frac{\delta}{w_c} \right) + p \left(\frac{\delta}{w_c} \right)^2 \right] \tag{1}$$

Eq. (1) describes the stress-crack width relationship for fiber-reinforced composites assuming frictional interfacial bond and taking into account the effect of fiber rupture (Maalej et al., in press, 1993). In (1), w_c represents the crack width at which the bridging stress vanishes, T_b represents the postcracking strength of the composite, k describes the magnitude of the initial slope of the tension softening curve, and p describes the rate at which the slope of the tension-softening curve decreases as a function of crack width. For instance, in the case of a linear tension-softening curve, k and p are equal to 1/2 and 0, respectively (since the slope of the tension softening curve is a constant and equal to T_b/w_c). The parameters w_c, T_b, k, and p depend on the composite micromechanical parameters and are defined in Appendix I.

If the crack is assumed to have a linear profile, then the crack width δ at any location x within the fracture process zone can be related to the crack mouth-opening w as follows:

$$\delta = w \left(1 - \frac{x}{a} \right) \tag{2}$$

Therefore, the distribution of normal stresses within the fracture process zone ($0 \le x \le a$) is given by

$$\sigma_1(x) = T_b \left[1 - 2ku \left(1 - \frac{x}{a} \right) + pu^2 \left(1 - \frac{x}{a} \right)^2 \right] \tag{3}$$

where $u = w/w_c$ = normalized crack mouth opening.

For a given crack length a, the crack mouth-opening w can be obtained essentially by solving a boundary value problem of a cracked linear elastic body as shown in Fig. 1. This yields a solution for the crack mouth opening w as a function of the externally applied moment M, stress distribution within the fracture process zone, crack length a, specimen geometry, and material property. The derivation in Appendix II yields the following implicit solution for the normalized crack mouth-opening u:

$$u = B\left(\left\{\frac{6M}{T_b b d^2} - r\left[3 - 3r + (2r - 3)ku + \left(1 - \frac{r}{2}\right)pu^2\right]\right\} V_1(r) - r\left(1 - ku + \frac{1}{3}pu^2\right) V_2(r)\right) \quad (4)$$

where $B = T_b d/(E_c w_c)$; and $r = a/d$. The parameter B is referred to as the brittleness ratio, and E_c is the Young's modulus of the composite. In addition, $V_1(r)$ and $V_2(r)$ are coefficients for compliance (with respect to crack mouth opening) of the cracked beam when subjected to a bending moment, and a uniformly applied stress, respectively (see Appendix II).

The crack length a can be related to the applied moment M and the stress distribution $\sigma_1(x)$ by specifying a crack-propagation criterion. In this case, the hypothesis of the FCM, that the crack propagates as soon as the stress at the crack tip exceeds the tensile strength of the material, is adopted. Furthermore, a linear stress distribution $\sigma_2(x)$ outside the fracture process zone with a maximum tensile stress T_c at the crack tip and a compressive stress C at the beam compressive face is assumed (see Fig. 1). Therefore, the distribution of normal stresses in the beam cross section where the fictitious crack resides is given by the following set of equations:

$$\sigma_1(x) = T_b\left[1 - 2ku\left(1 - \frac{x}{a}\right) + pu^2\left(1 - \frac{x}{a}\right)^2\right] \quad \text{for } 0 \le x \le a \quad (5)$$

$$\sigma_2(x) = \frac{1}{d - a}\left[T_c(d - x) - C(x - a)\right] \quad \text{for } a \le x \le d \quad (6)$$

Note that the tensile strength T_c is equal to the first cracking strength, and it is assumed greater or equal to postcracking strength T_b. The crack length a (or normalized crack length r) can now be related to the applied moment M and the stress distribution $\sigma_1(x)$ by writing the equilibrium equations for the beam section shown in Fig. 1, namely, the sum of normal forces is equal to zero and the moment of the normal forces is equal to the external bending moment M

$$\int_0^a b\sigma_1(x)\,dx + \int_a^d b\sigma_2(x)\,dx = 0 \quad (7)$$

$$\int_0^a b\sigma_1(x)x\,dx + \int_a^d b\sigma_2(x)x\,dx = M \quad (8)$$

Solving (7) and (8) for M and C, the following equations are obtained:

$$M = \frac{T_c b d^2}{6}\left\{(1 - r)^2 + \alpha r\left[4 - r - 4ku + p\left(\frac{4}{3} + \frac{r}{6}\right)u^2\right]\right\} \quad (9)$$

$$C = T_c\left[1 + \frac{2\alpha r}{(1 - r)}\left(1 - ku + \frac{1}{3}pu^2\right)\right] \quad (10)$$

where $\alpha = T_b/T_c$. Written in normalized form, M becomes

$$q = \frac{6M}{T_c b d^2} = (1 - r)^2 + \alpha r\left[4 - r - 4ku + p\left(\frac{4}{3} + \frac{r}{6}\right)u^2\right] \quad (11)$$

Substituting M from (9) into (4) and solving for u, the following equation is obtained:

$$u = u(B, \alpha, k, p, r) = \frac{1}{8}\left[\frac{12k}{p} + \frac{3}{Bpr^2[V_1(r)(1 + 2r) - V_2(r)]} - \left(\frac{192}{p}\left\{\frac{V_1(r)(1 - r)^2}{\alpha r[V_2(r) - V_1(r)(1 + 2r)]} - 1\right\} + \left\{\frac{12k}{p} + \frac{3}{Bpr^2[V_1(r)(1 + 2r) - V_2(r)]}\right\}^2\right)^{0.5}\right] \quad (12)$$

The normalized-crack mouth-opening u can be substituted in (11) to obtain q. Thus

$$q(B, \alpha, k, p, r) = (1 - r)^2 + \alpha r\left[4 - r - 4ku(B, \alpha, k, p, r) + p\left(\frac{4}{3} + \frac{r}{6}\right)u(B, \alpha, k, p, r)^2\right] \quad (13)$$

The normalized moment q reaches a maximum value q_u at some critical value r_c of r between 0 and 1. This corresponds to a partially developed fracture process zone. For known tensile properties of a material and specimen geometry (B, α, k, and p are known), the normalized flexural strength can be deduced by computing the maxima of $q(B, \alpha, k, p, r)$. Therefore, the normalized flexural strength is given by

$$q_u(B, \alpha, k, p) = q(B, \alpha, k, p, r_c) \quad (14)$$

where $\partial q/\partial r\ (r = r_c) = 0$. In general, the compressive stress $C(B, \alpha, k, p, r_c, T_c)$ is less than the compressive strength of the material C_c, however, this should always be confirmed when using (14). In the case when $C(B, \alpha, k, p, r_c, T_c)$ is greater than C_c, the normalized flexural strength will be given by $q(B, \alpha, k, p, r_c')$, where $C(B, \alpha, k, p, r_c', T_c)$ is equal to C_c.

The normalized flexural strength q_u can be written as follows:

$$q_u = \frac{(6M_u/bd^2)}{T_c} = \frac{MOR}{T_c} \quad (15)$$

where M_u and MOR = ultimate moment capacity and modulus of rupture, respectively. Hence, q_u is the ratio of flexural strength to tensile strength (T_c).

RESULTS AND ANALYSIS

Fig. 2 shows the variation of the flexural strength to tensile strength ratio q_u as a function of the brittleness ratio B for the case in which no fiber rupture occurs in the composite and the first cracking strength is equal to the postcracking strength (i.e., $\alpha = k = p = 1$). It can be seen from this figure that q_u decreases with an increasing brittleness ratio. In the limiting case when B is infinite, corresponding to linear elastic brittle behavior of the material, the flexural strength is equal to the tensile strength as predicted by the linear elastic brittle theory. In the other limiting case, $B \to 0$, the

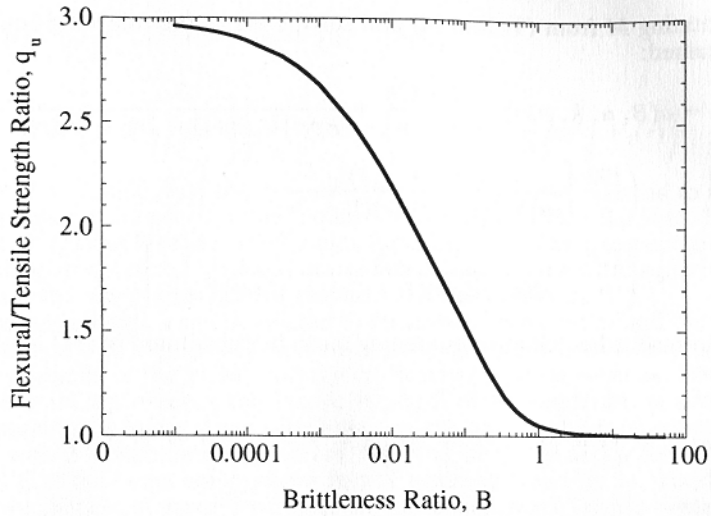

FIG. 2. Variation of Flexural Strength/Tensile Ratio as Function of Brittleness Ratio

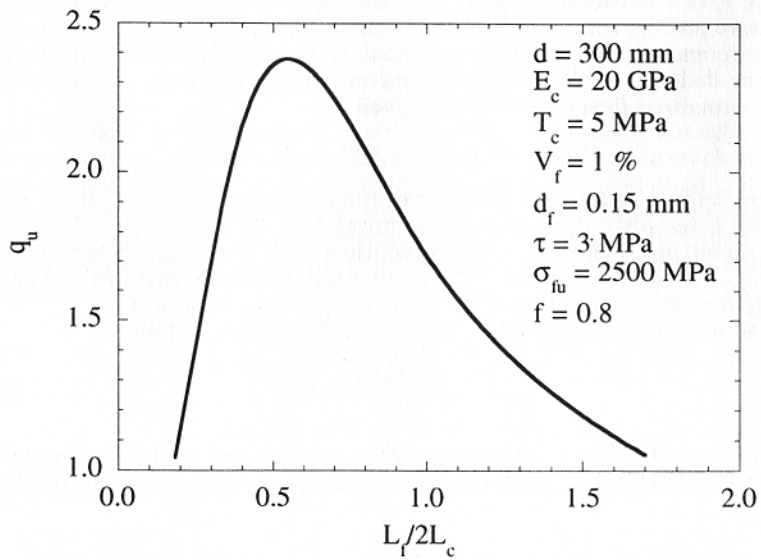

FIG. 3. Variation of Flexural Strength to Tensile Strength Ratio as Function of Fiber Length

ratio of flexural strength to tensile strength is equal to 3, as predicted by plastic theory.

Fig. 3 shows the variation of the flexural strength to tensile strength ratio q_u as a function of fiber length for a typical fiber-reinforced composite. This figure indicates that q_u increases initially as a function of fiber length, reaches an optimum value, and then starts to decrease as the fiber length continues

to increase. The drop in q_u is due to fiber rupture that reduces the stress acting across the fracture-process zone. Alternatively, the energy consumed due to fiber frictional pullout is known to diminish with fiber length when fiber rupture occurs (Li et al. 1991). Therefore, it is deduced that an optimum fiber length exists at which the ratio of flexural strength to tensile strength is optimum.

Eq. (14) can be used to predict the flexural strength of any fiber-reinforced cementitious composite based on the knowledge of either its micromechanical parameters or its tension-softening relationship (in either case B, α, k, and p would be known). In addition, (14) can be used to perform a parametric study on the flexural strength of any fiber-reinforced composite. This allows an understanding of how the flexural strength of fiber-reinforced composites depends on the different micromechanical parameters, so that the flexural strength can be controlled by the micromechanical parameters. Ideally the micromechanical parameters would be selected such that the required flexural strength (for a particular application) is met using the minimum fiber-volume fraction. In this case, for a given fiber-volume fraction, fiber tensile rupture strength, and beam geometry, the selected micromechanical parameters would give the highest flexural strength and any attempt to change the micromechanical parameters (such as an increase or decrease of fiber length, fiber diameter, frictional bond strength, or snubbing friction coefficient) would result in decreasing the flexural strength. Whether a given fiber composite can be made to achieve its optimum flexural strength depends on the feasible range of the micromechanical parameters, given the state of technology. For example, fiber length can be easily customized and controlled. However, material processing can become a problem when long fibers are required for optimum performance. In addition, fiber/matrix interfacial bond strength can be adjusted, for instance, through surface finish modification and/or mechanical crimping (Wang et al. 1991).

Fig. 4 shows the variation of flexural strength as a function of beam depth, as predicted by the proposed model and experimentally measured by Ward and Li (1990) for an aramid fiber-reinforced mortar. The fiber volume fraction was 1.5%, and the beam depths were 63.5, 114, 171, and 228 mm. The dimensions and mechanical properties of the aramid fibers are shown in Table 1. The tensile strength of the composite was measured to be 4.6 MPa. The model assumed a Young's modulus of 20 GPa for the composite, and a snubbing friction coefficient of 0.95 (within typical range). The critical fiber length for this composite ($2L_c$, see Appendix I) is 3.6 mm. This indicates that the composite must have failed with a large fraction of ruptured fibers within the beam-fracture process zone. Fig. 4 shows that there is a reasonable agreement between the experimental data and the theoretical prediction for the composite flexural strength. The model and experimental data suggest that the flexural strength decreases as the depth of the beam increases. This trend of decreasing flexural strength with increasing beam depth has also been experimentally recorded for plain concrete (Hillerborg et al. 1976; Torrent and Brooks 1985) and fiber reinforced concrete (Johnston 1982).

Johnston (1982) studied the effect of beam depth on the flexural strength of steel fiber-reinforced concrete. The fiber volume fraction was 1.14% and the beam depths were 75, 100, and 150 mm. The dimensions of the steel fibers are shown in Table 1. The experimental results along with the model prediction are shown in Fig. 5. The tensile strength of the composite was assumed equal to the postcracking strength (i.e., $\alpha = 1$) and the Young's

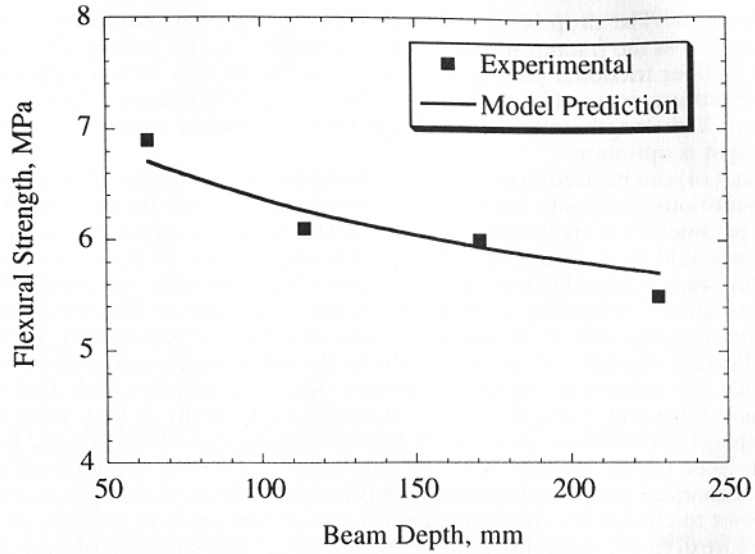

FIG. 4. Effect of Beam Depth on Flexural Strength of Aramid Fiber-Reinforced Mortar

TABLE 1. Dimensions and Mechanical Properties of Fibers

Fiber (1)	L_f (mm) (2)	d_f (mm) (3)	σ_{fu} (MPa) (4)	τ (MPa) (5)	f (6)
Aramid	6.4[a]	0.012[a]	2800[a]	4.5[b]	0.95[c]
Steel	25[d]	0.344[e]	—	2.9[c]	0.80[c]

[a]Ward and Li (1990).
[b]Wang (1989).
[c]Assumed.
[d]Johnston (1982).
[e]Equivalent diameter $2ab/(a + b)$, where a (0.25 mm) and b (0.55 mm) are dimensions of fiber rectangular x-section.

modulus of the composite was assumed to be 25 GPa. In addition, no fiber rupture was assumed to take place in the composite. Fig. 5 shows a reasonable agreement between the model prediction and the experimental data. Both suggest that the flexural strength decreases as the beam depth increases.

For the case of no fiber rupture in the composite the brittleness ratio B is equal to $d/(3l_{ch})$, where l_{ch} is referred to as the characteristic length (Hillerborg 1986) and is defined as follows:

$$l_{ch} = \frac{G_b E_c}{T_b^2} \tag{16}$$

where G_b = composite bridging toughness that can be computed by integrating the area under the tension-softening curve. The characteristic length l_{ch} is a material property that has no direct physical meaning, but it is a

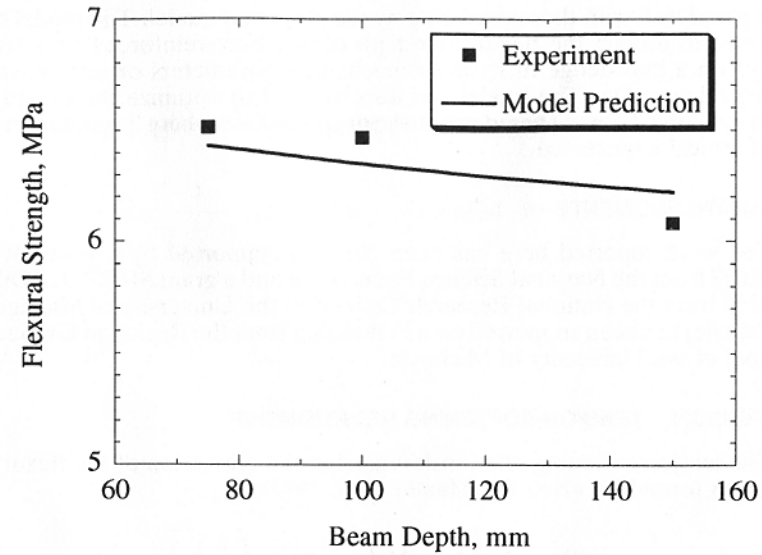

FIG. 5. Effect of Beam Depth on Flexural Strength of Steel Fiber-Reinforced Concrete

parameter that determines the size of the process zone at ultimate load. Hillerborg (1986) indicated that the flexural strength of steel fiber-reinforced concrete depends significantly on the initial slope of the tension-softening curve. Therefore, Hillerborg defined an effective characteristic length l'_{ch} based on the area G'_b under the continuation of the tension-softening-curve initial slope. In addition, Hillerborg suggested that the area under the tension-softening curve, at large crack openings, has little influence on the beam flexural strength. The proposed model shows that this is indeed the case. According to the model, the flexural strength of fiber-reinforced composites is always reached before the crack mouth opening reaches $w_c/5$. In particular, for small values of the brittleness ratio ($B \to 0$) the flexural strength is reached when the crack mouth opening is very small ($u \to 0$), and the fracture process zone has extended close to the full beam depth ($r \to 1$). In this case, the cohesive stress acting across the process zone is almost a constant and equal to the postcracking strength T_b. When the tensile strength is equal to the postcracking strength (i.e., $\alpha = 1$), the described condition leads to a ratio of flexural strength to tensile strength close to 3.

CONCLUSIONS

This paper presents a theoretical model for the flexural strength of fiber-reinforced cement-based materials. From this model it can be deduced that the flexural strength is dependent on specimen geometry and is also strongly influenced by the stress acting across the process zone. In addition, the flexural strength is always higher than the tensile strength and it is reached when the fracture process zone is only partially developed. The trend of decreasing flexural strength with beam depth, as experimentally measured for an aramid fiber reinforced mortar and a steel fiber-reinforced concrete,

compared well with those predicted by the proposed model. The model can be used to predict the flexural strength of any fiber-reinforced composite based on a knowledge of its micromechanical parameters or tension-softening relationship. The model can also be used to optimize the design of fiber-reinforced cement based materials for applications where flexural strength is of critical importance.

ACKNOWLEDGMENTS

The work reported here has been partially supported by a grant BCS-9202097 from the National Science Foundation and a grant SHRP-91-ID036 030219 from the National Research Council to the University of Michigan. M. Maalej has been supported on a Fellowship from the Rackham Graduate School of the University of Michigan.

APPENDIX I. TENSION-SOFTENING RELATIONSHIP

The tension-softening relationship used in the derivation of the flexural-strength formula is given by (Maalej et al. 1993)

$$\sigma(\delta) = T_b\left[1 - 2k\left(\frac{\delta}{w_c}\right) + p\left(\frac{\delta}{w_c}\right)^2\right] \tag{17}$$

where

$$T_b = \begin{cases} g\sigma_o & \text{for } L_f \le 2L_c e^{-f\pi/2} \quad (18a) \\ [g(\Phi_b) + b(-f)\hat{L}_c^2]\sigma_o & \text{for } 2L_c e^{-f\pi/2} \le L_f \le 2L_c \quad (18b) \\ g_1\hat{L}_c^2\sigma_o & \text{for } L_f \ge 2L_c \quad (18c) \end{cases}$$

$$k = \begin{cases} 1 & \text{for } L_f \le 2L_c e^{-f\pi/2} \quad (19a) \\ \dfrac{g(\Phi_b) + b(0)\hat{L}_c}{g(\Phi_b) + b(-f)\hat{L}_c^2} & \text{for } 2L_c e^{-f\pi/2} \le L_f \le 2L_c \quad (19b) \\ \dfrac{1}{g_1} & \text{for } L_f \ge 2L_c \quad (19c) \end{cases}$$

$$p = \begin{cases} 1 & \text{for } L_f \le 2L_c e^{-f\pi/2} \quad (20a) \\ \dfrac{g}{g(\Phi_b) + b(-f)\hat{L}_c^2} & \text{for } 2L_c e^{-f\pi/2} \le L_f \le 2L_c \quad (20b) \\ \dfrac{g}{g_1} & \text{for } L_f \ge 2L_c \quad (20c) \end{cases}$$

$$w_c = \begin{cases} \dfrac{L_f}{2} & \text{for } L_f \le 2L_c \quad (21a) \\ L_c & \text{for } L_f \ge 2L_c \quad (21b) \end{cases}$$

$$g = \frac{2}{4 + f^2}(1 + e^{f\pi/2}) \tag{22}$$

$$\sigma_o = \frac{V_f \tau L_f}{2d_f} \tag{23}$$

$$g(\Phi_b) = \frac{1}{4 + f^2}\{[f\sin(2\Phi_b) - 2\cos(2\Phi_b)e^{f\Phi_b} + 2\} \tag{24}$$

$$b(t) = \frac{1}{4 + t^2}\{[2\cos(2\Phi_b) - t\sin(2\Phi_b)]e^{t\Phi_b} + 2e^{t\pi/2}\} \tag{25}$$

$$\Phi_b = \frac{1}{f}\ln(\hat{L}_c) \tag{26}$$

$$\hat{L}_c = \frac{2L_c}{L_f} \tag{27}$$

$$L_c = \frac{\sigma_{fu} d_f}{4\tau} \tag{28}$$

$$g_1 = \frac{2}{4 + f^2}(1 + e^{-f\pi/2}) \tag{29}$$

It should be noted that in the case of no fiber rupture ($L_f \le 2L_c e^{-f\pi/2}$), (17) describes the complete tension-softening curve. However, in the case of fiber rupture ($L_f \ge 2L_c e^{-f\pi/2}$), (17) describes only the initial portion of the tension-softening curve ($\delta \le L_c e^{-f\pi/2}$), which was found to govern the flexural strength of the composite. Fig. 6 shows the variation of k, p, and T_b as a function of the normalized fiber length for a snubbing friction coefficient of 0.8.

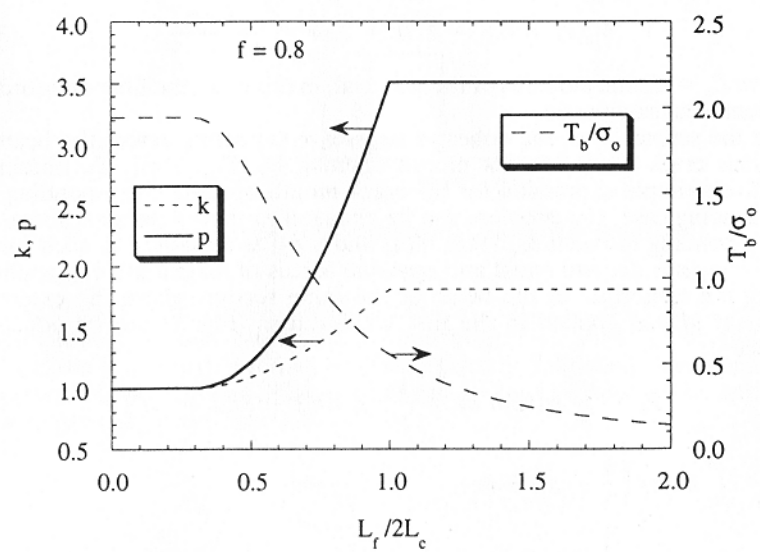

FIG. 6. Variation of T_b, k, and p as Function of Normalized Fiber Length

APPENDIX II. DERIVATION OF CRACK MOUTH OPENING

In principle, the assumption of a linear crack profile to approximate the stress distribution within the fracture process zone $\sigma[\delta(x)]$ is not necessary. In fact, the crack profile $\delta(x)$ can be computed in the manner suggested by Tada et al. (1985), except, the solution will involve the evaluation of an integral where $\sigma[\delta(x)]$ is part of the integrand. Therefore, an analytical solution for $\delta(x)$ (and therefore $\sigma[\delta(x)]$) cannot be obtained. In addition, the equilibrium equations (7) and (8) involve a further integration of the stress distribution $\sigma[\delta(x)]$. Consequently, an explicit solution for the moment M as a function of the crack size, specimen geometry, and material property would be impossible. By making the simplifying assumption of a linear crack profile, the stress distribution within the fracture process zone would be known $\{\sigma[\delta(x)] = \sigma_1(x)\}$ if the crack mouth-opening w can be determined.

Using the principle of superposition, the crack mouth opening w can be computed as a function of the external bending moment M and the stress distribution σ_1 within the fracture-process zone. The problem of solving for the crack mouth opening w can be separated into two different cases as shown in Fig. 7. The algebraic sum of the two crack mouth openings caused by the separate loads M and σ_1 (viewed as an externally applied load) gives the total crack mouth opening.

In the first case, the external bending moment M, applied to the beam where there are no cohesive forces acting across the fictitious crack, causes a crack mouth opening w_1 [Fig. 7(*b*)]. Tada et al. (1985) give the following expression for the crack mouth opening caused by a bending moment applied to a single-edge notch specimen:

$$w_1 = \frac{24Ma}{bd^2E_c} V_1\left(\frac{a}{d}\right) = \frac{24Mr}{bdE_c} V_1(r) \tag{30}$$

where

$$V_1(r) = 0.8 - 1.7r + 2.4r^2 + \frac{0.66}{(1 - r)^2} \tag{31}$$

where E_c = elastic modulus of the material, in this case, the fiber-reinforced cementitious composite.

In the second case, the cohesive stresses $\sigma_1(x)$ acting across the beam's ficitious crack cause a crack mouth opening w_2 [Fig. 7(*c*)]. To obtain a relatively simple expression for the crack mouth opening corresponding to this loading case, the problem can be changed to that of an axial force F_σ and a bending moment M_σ [Figs. 8(*a*) and 8(*b*)] as follows: For each force $dF_\sigma = \sigma_1(x)b\,dx$, two equal and opposite forces of magnitude dF_σ applied along the centerline of the beam at the same section where the external moment M was applied in the first loading case (Fig. 9) are introduced. Hence

$$F_\sigma = \int_0^a \sigma_1(x)b\,dx = \frac{1}{3} T_b b\,dr(3 - 3ku + pu^2) \tag{32}$$

$$M_\sigma = \int_0^a \sigma_1(x)\left(\frac{d}{2} - x\right) b\,dx$$

$$= \frac{1}{12} T_b bd^2r(6 - 6r - 6ku + 4kru + 2pu^2 - pru^2) \tag{33}$$

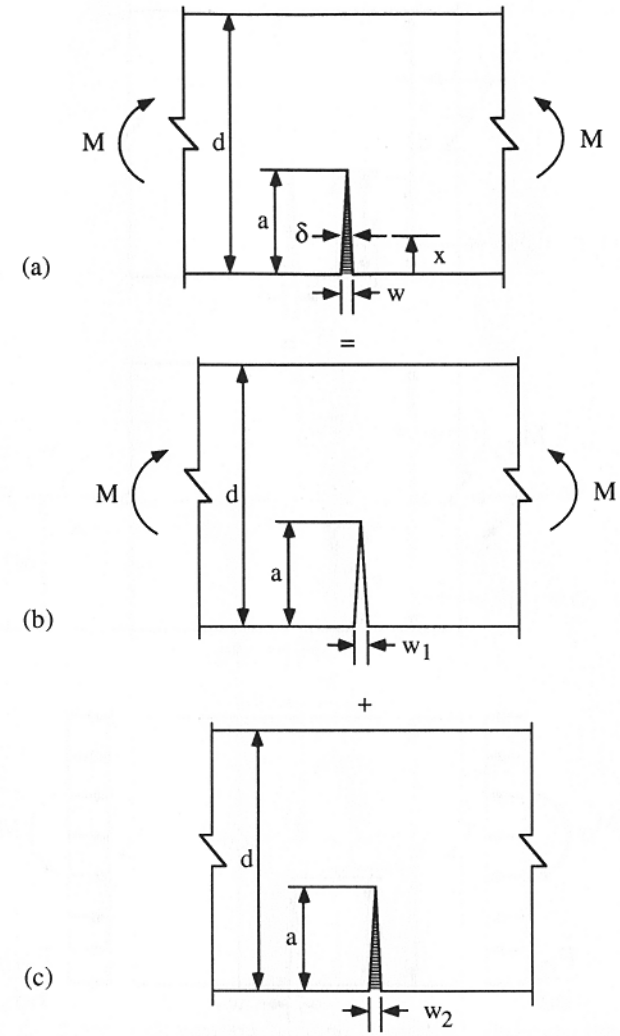

FIG. 7. Superposition of Crack Mouth-Opening Displacements

The crack mouth opening displacement w_{2F} due to the force F_σ can be approximated by that caused by a uniform applied stress of magnitude $\sigma = F_\sigma/bd$ [Fig. 8(*c*)]. Tada et al. (1985) give the following expression for the crack mouth opening displacement caused by a uniform stress applied to a single-edge notch specimen:

$$w_{2F} = -\frac{4\sigma a}{E_c} V_2\left(\frac{a}{d}\right) = -\frac{4F_\sigma r}{bE_c} V_2(r) \tag{34}$$

where

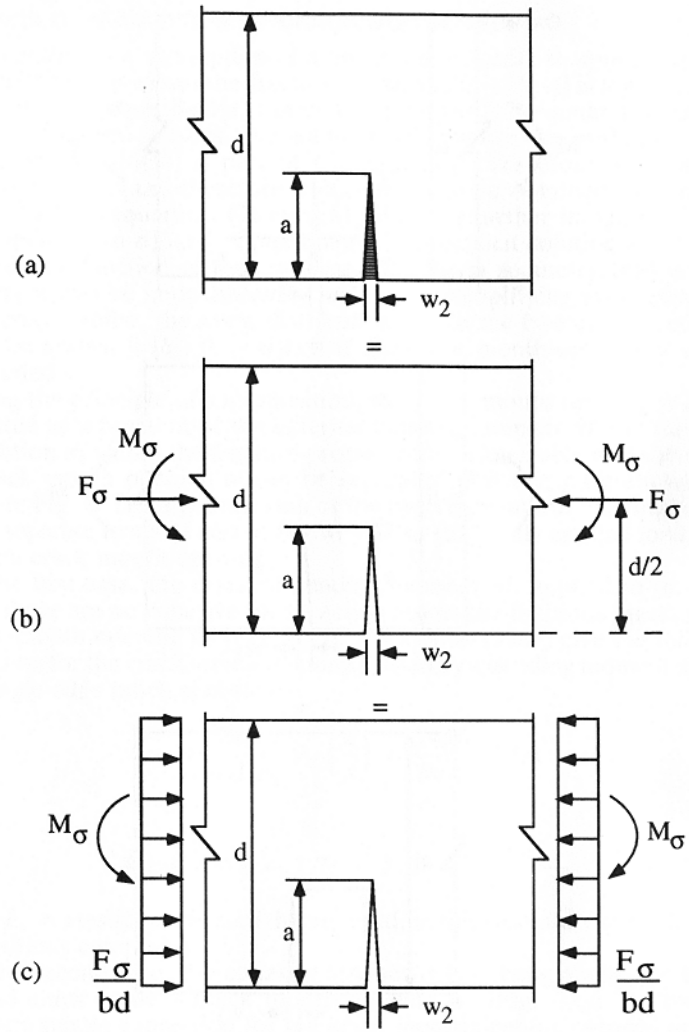

FIG. 8. Approximation of Crack Mouth-Opening Displacement Caused by Cohesive Forces Action

$$V_2(r) = \frac{1.46 + 3.42\left[1 - \cos\left(\frac{\pi}{2}r\right)\right]}{\left[\cos\left(\frac{\pi}{2}r\right)\right]^2} \tag{35}$$

Similar to the first loading case, the crack mouth opening displacement w_{2M} caused by the moment M_σ is given by

$$w_{2M} = -\frac{24M\sigma r}{bdE_c}V_1(r) \tag{36}$$

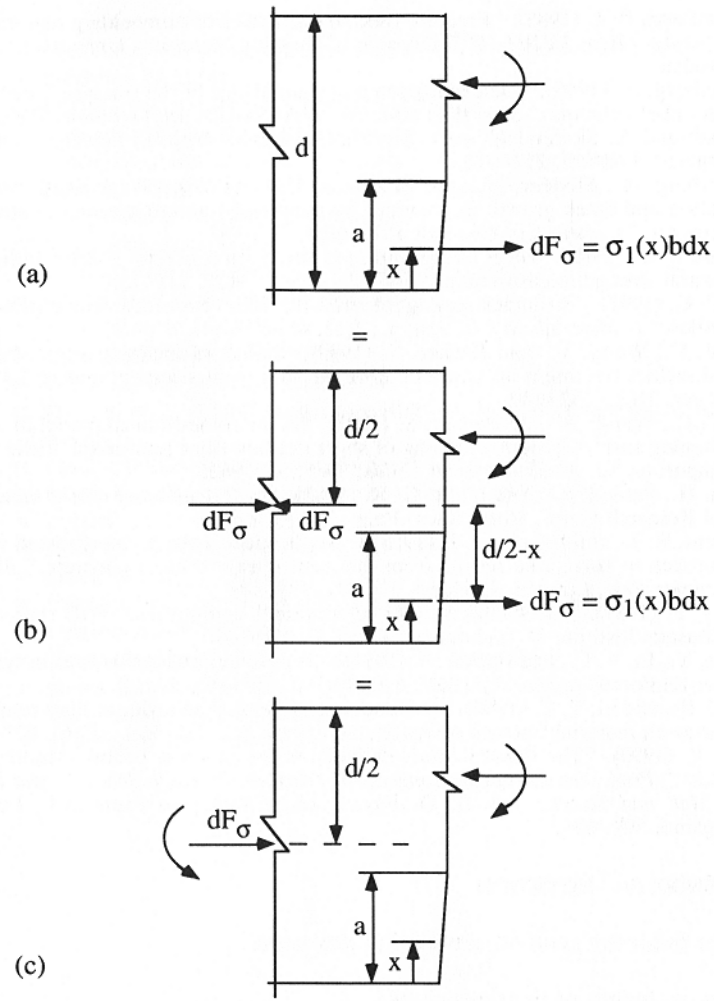

FIG. 9. Steps in Computing Bending Moment M_σ and Axial Force F_σ

Hence

$$w = w_c u = w_1 + w_2 = w_1 + (w_{2F} + w_{2M})$$

$$= \frac{4r}{bE_c}\left[\frac{6}{d}(M - M_\sigma)V_1(r) - F_\sigma V_2(r)\right] \tag{37}$$

Substituting M_σ and F_σ, from (32) and (33), respectively, in (37), we obtain (4).

APPENDIX III. REFERENCES

Bažant, Z. (1992). "Should design codes consider fracture mechanics size effect?" *Concrete Design Based on Fracture Mechanics, ACI SP-134*, American Concrete Institute, Detroit, Mich., 1–24.

Gustafsson, P. J. (1985). "Fracture mechanics studies of nonyielding materials like concrete." *Rep. TVBM-1007*, Division of Building Materials, University of Lund, Sweden.
Hillerborg, A. (1986). "Determination and significance of the fracture toughness of steel fiber concrete." *Steel fiber concrete (U.S.-Sweden joint seminar, 1985)*, S. P. Shah and A. Skarendahl, eds., Stockholm/Elsevier Applied Science Publishers, England, London, 257–271.
Hillerborg, A., Modéer, M., and Petersson, P. E. (1976). "Analysis of crack formation and crack growth in concrete by means of fracture mechanics and finite elements." *Cement and Concrete Res.*, 6(6), 773–782.
Johnston, D. (1982). "Steel fiber reinforced and plain concrete: Factors influencing flexural strength measurement." *ACI J., Proc.*, 79(2), 131–138.
Li, V. C. (1992). "Postcrack scaling relations for fiber reinforced cementitious composites." *J. Materials in Civ. Engrg.*, 4(1), 41–57.
Li, V. C., Wang, Y., and Backer, S. (1990). "Effect of inclining angle, bundling and surface treatment on synthetic fibre pull-out from a cement matrix." *J. Composites*, 21(2), 132–140.
Li, V. C., Wang, Y., and Backer, S. (1991). "A micromechanical model of tension softening and bridging toughening of short random fiber reinforced brittle matrix composites." *J. Mech. Physical Solids*, 39(5), 607–625.
Tada, H., Paris, P. C., and Irwin, G. R. (1985). *Stress analysis of cracks handbook*. Del Research Corp., Hellertown, Pa.
Torrent, R. J., and Brooks, J. J. (1985). "Application of the highly stressed volume approach to correlated results from different tensile tests of concrete." *Mag. of Concrete Res.*, London, England, 37(132), 175–184.
Wang, Y. (1989). "Mechanics of fiber cementitious composites," PhD thesis, Massachusetts Institute of Technology, Cambridge, Mass.
Wang, Y., Li, V. C., and Backer, S. (1991). "Tensile failure mechanisms in synthetic fiber-reinforced mortar." *J. Mat. Sci.*, 26(24), 6565–6575.
Ward, R., and Li, V. C. (1990). "Dependence of flexural behavior of fiber reinforced mortar on material fracture resistance and beam size." *J. Mat.*, 87(6), 627–637.
Zhu, Y. (1990). "The flexural strength function for concrete beams without initial cracks." *Proc., 8th European Congress of Fracture: Fracture Behavior and Design of Mat. and Struct.; Vol. II*, D. Firrao, ed., Chameleon Press Ltd., London, England, 599–604.

APPENDIX IV. NOTATION

The following symbols are used in this paper:

a = length of fictitious crack;
B = brittleness ratio;
b = beam width;
C = compressive stress at beam-compressive face;
C_c = composite-compressive strength;
d = beam depth;
d_f = fiber diameter;
E_c = Young's modulus of composite;
F_σ = equivalent axial force due to crack-cohesive stresses $\sigma_1(x)$;
f = snubbing friction coefficient;
G_b = composite bridging toughness;
k, p = parameters that describe shape of tension-softening curve;
L_c = half-critical fiber length;
L_f = fiber length;
l_{ch} = characteristic length;
M = externally applied moment;

M_u = ultimate moment capacity;
M_σ = equivalent bending moment due to crack-cohesive stresses $\sigma_1(x)$;
MOR = modulus of rupture;
q = normalized externally applied moment;
r = normalized length of fictitious crack;
r_c = normalized length of fictitious crack at ultimate moment capacity;
q_u = ratio of flexural strength to tensile strength;
T_b = composite postcracking strength;
T_c = composite tensile strength;
t = dummy variable that takes values of 0, and $-f$;
u = normalized crack mouth opening;
V_f = fiber volume fraction;
w = total crack mouth opening;
w_1 = crack mouth opening due to M;
w_2 = $(w_{2F} + w_{2M})$ crack mouth opening due to crack-cohesive stresses $\sigma_1(x)$;
w_{2F} = crack mouth opening due to axial force F_σ;
w_{2M} = crack mouth opening due to bending moment M_σ;
w_c = critical crack mouth opening;
α = ratio of postcracking strength to tensile strength;
δ = crack width;
Φ = fiber inclination angle with respect to loading direction;
$\sigma(\delta)$ = tension-softening relationship;
$\sigma_1(x)$ = stress distribution within fracture process zone;
$\sigma_2(x)$ = stress distribution outside fracture process zone;
σ_{fu} = fiber tensile strength; and
τ = interfacial frictional bond strength.